



ELSEVIER

Diphenyl-2-pyridylphosphine as a bidentate ligand in the coordination of dicobalt octacarbonyl; X-ray crystal structures of $\text{Co}_2(\text{CO})_4(\mu\text{-}P,N\text{-PPh}_2\text{py})\{\mu\text{-HC}\equiv\text{CSiMe}_3\}$, and $\text{Co}_4(\text{CO})_{10}(\mu\text{-}P,N\text{-PPh}_2\text{py})$

Fung-E. Hong ^{a,*}, Yu-Chang Chang ^a, Ruei-E. Chang ^a, Chu-Chieh Lin ^a,
Sue-Lein Wang ^b, Fen-Ling Liao ^b

^a Department of Chemistry, National Chung-Hsing University, Taichung 40227, Taiwan, ROC

^b Department of Chemistry, National Tsing-Hua University, Hsinchu 30043, Taiwan, ROC

Received 19 December 1998; received in revised form 22 June 1999

Abstract

Under mild conditions, the reaction of $\text{Co}_2(\text{CO})_8$ with $\text{HC}\equiv\text{CSiMe}_3$ in the presence of PPh_2py gave a binuclear cobalt carbonyl complex, $\text{Co}_2(\text{CO})_4(\eta^2\text{-}\mu_2\text{-HC}\equiv\text{CSiMe}_3)(\mu\text{-PPh}_2\text{py})$ (**1a**), which has both zero-valent cobalt centers coordinated by a bidentate ligand, PPh_2py . PPh_2py is also an effective ligand in promoting the yield of 2,5-bis(trimethylsilyl) cyclopenta-2,4-dien-1-one. A cobalt cluster complex, $\text{Co}_4(\text{CO})_{10}(\mu\text{-}P,N\text{-PPh}_2\text{py})$ (**9**) was obtained when two equivalents of $\text{Co}_2(\text{CO})_8$ were reacted with PPh_2py at a higher temperature. The phosphorus and nitrogen atoms of the ligand coordinate to cobalt in the basal and apical positions, respectively. These two compounds, **1a** and **9** were characterized by spectroscopic means as well as X-ray crystal structure determination. © 1999 Elsevier Science S.A. All rights reserved.

Keywords: Bidentate-ligand; μ -Alkyne-bridged; Bimetallic compounds; Cobalt cluster

1. Introduction

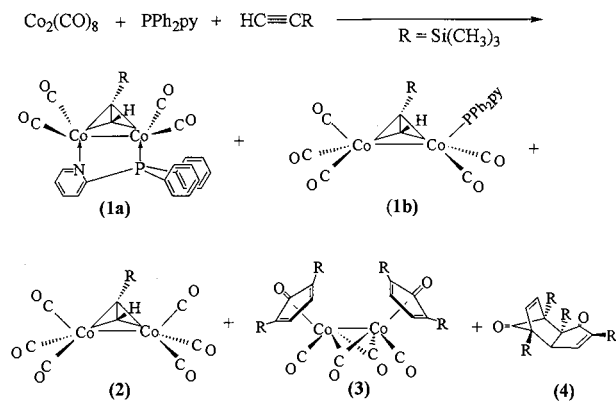
Pyridylphosphine has been used as a multi-dentate ligand to coordinate transition metals. The study of such use has recently attracted much attention [1]. The labile nitrogen–metal bond of the pyridyl-coordinated metal center is a useful quality in various catalytic reactions involving pyridylphosphine as a bi- or multi-dentate ligand [2]. Many examples of pyridylphosphine-coordinated bimetallic compounds are known [3]. Nevertheless, only one structure among all the diphenyl-2-pyridylphosphine-coordinated bimetallic compounds has been reported so far [1f]. One of the reasons for this is the relatively rigid bond distance, approximately 2.7 Å, between the nitrogen and phosphorus atoms ($\text{P}\cdots\text{N}$) of pyridylphosphine. Normally, the bond lengths between two cobalt atoms in a dicobalt system are within the range 2.4–2.5 Å. This is an appropriate distance for the coordination to take place with only a slight twist of the

ligand. A crystal structure of a diphenyl-2-pyridylphosphine-coordinated mixed-valence complex, $\text{Co}^0\text{Co}^{\text{I}}(\mu\text{-PPh}_2\text{py})_2(\mu\text{-CO})(\text{CO})\text{Cl}$, was reported [1f]. The phosphorus atom and the nitrogen atom of the ligand bridge to the $\text{Co}(0)$ atom and the $\text{Co}(\text{I})$ atom, respectively. This result is consistent with the prediction of HSAB theory [4]. In this paper, we shall report the preparations and characterizations of the diphenyl-2-pyridylphosphine-coordinated di- and tetra-cobalt systems. These systems both have zero-valence cobalt atoms. Trimethylamine *N*-oxide (TMNO) is a powerful decarbonyl reagent and has been extensively used in the synthesis of various organometallic compounds [5]. Results from similar reactions with the presence of TMNO and different phosphines are reported here for comparison.

2. Results and discussion

The reaction of $\text{Co}_2(\text{CO})_8$ with trimethylsilylacetylene in the presence of diphenyl-2-pyridylphosphine at 60°C

* Corresponding author. Fax: +886-4-2862547.



Scheme 1.

yielded two desired major compounds, $\text{Co}_2(\text{CO})_4(\mu\text{-P}, \text{N}\text{-PPh}_2\text{py})\{\mu\text{-HC}\equiv\text{CSiMe}_3\}$ (**1a**) and $\text{Co}_2(\text{CO})_5\text{-}(\text{PPh}_2\text{py})\{\mu\text{-HC}\equiv\text{CSiMe}_3\}$ (**1b**) (Scheme 1). The yields of **1a** and **1b** are both about 15%. Both **1a** and **1b** are characterized by spectroscopic means (Table 1); the crystal structure of **1a** was determined as well. Three known compounds, $\text{Co}_2(\text{CO})_6\{\mu\text{-HC}\equiv\text{CSiMe}_3\}$ (**2**), $\text{Co}_2(\text{CO})_2(\mu\text{-CO})_2(\eta^4\text{-}2,5\text{-bis}(\text{trimethylsilyl})\text{cyclopentadienone})_2$ (**3**) and 2,5-bis(trimethylsilyl)cyclopent-2,4-dien-1-one (**4**), were obtained along with **1a** and **1b**.

Our previous work has shown that the reaction of $\text{Co}_2(\text{CO})_8$ with trimethylsilylacetylene in the presence of triphenylphosphine yielded two dinuclear cobalt carbonyls, $\text{Co}_2(\text{CO})_3(\text{PPh}_3)\{\mu\text{-C}(\text{SiMe}_3)=\text{CH}-\text{CH}=\text{C}(\text{SiMe}_3)-\text{CH}=\text{C}(\text{SiMe}_3)\}$ (**5**) and (**3**) (Scheme 2) [6]. Both structures of **5** and **3** were determined by X-ray crystallographic methods. A rather small quantity of **3** was obtained until a 5:1 ratio of acetylene to $\text{Co}_2(\text{CO})_8$ was used [7]. It also showed that the oxidation of **3** in solution produced **4** quantitatively. There are several notable distinctions between the reactions shown in Schemes 1 and 2. Compound **4** was obtained while 1.5 equivalent of trimethylsilylacetylene was used and in the presence of PPh_2py ; on the contrary, no **4** was found under similar reaction conditions in Scheme 2. The distinct observations suggest that the bidentate ligand, diphenyl-2-pyridylphosphine, indeed promotes the formation of **3** which eventually converts to **4**. Another notable observation is the absence of **5** in Scheme 1, which is in contrast to the reaction in Scheme 2.

Trimethylamine *N*-oxide (TMNO) is a useful decarbonyl reagent. The reaction of **2** with PPh_2py in the presence of TMNO was pursued. By the assistance of TMNO, the reaction was carried out at room temperature. Under that reaction condition, only **1a** and **1b** were observed. The yield of **1a** was up to 45%. It was a more efficient way to obtain **1a**.

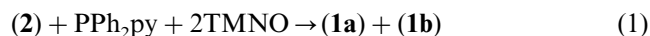


Table 1
Crystal data of **1a** and **9**

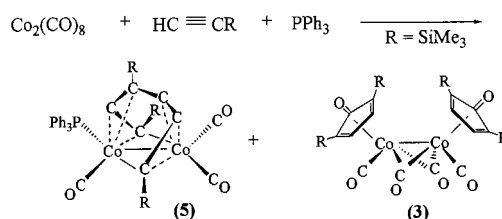
	$\text{C}_{26}\text{H}_{24}\text{Co}_2\text{NO}_4\text{PSi}$	$\text{C}_{27}\text{H}_{14}\text{Co}_4\text{NO}_{10}\text{P}$
Formula	$\text{C}_{26}\text{H}_{24}\text{Co}_2\text{NO}_4\text{PSi}$	$\text{C}_{27}\text{H}_{14}\text{Co}_4\text{NO}_{10}\text{P}$
Formula weight	591.38	779.1
Crystal system	Triclinic	Triclinic
Space group	$P\bar{1}$	$P\bar{1}$
<i>a</i> (Å)	10.59960(10)	9.792(1)
<i>b</i> (Å)	11.84370(10)	10.513(1)
<i>c</i> (Å)	12.1732(2)	14.573(2)
α (°)	80.2510(10)	83.65(1)
β (°)	85.3840(10)	87.58(1)
γ (°)	65.1030(10)	81.45(1)
<i>V</i> (Å ³)	1366.09(3)	1473.9(3)
<i>Z</i>	2	2
<i>D</i> _{calc.} (Mg m ⁻³)	1.438	1.755
λ (Mo-K α) (Å)	0.71073	0.71073
μ (mm ⁻¹)	1.347	2.322
Range (°)	1.7–27.94	4.0–50.0
Scan type	2 θ / θ	2 θ / θ
No. of reflections collected	13154	5511
No. of independent reflections	5834	5179
	(<i>R</i> _{int} = 3.76%)	(<i>R</i> _{int} = 0.92%)
No. of observed reflections		4451 (<i>F</i> > 4.0 σ (<i>F</i>))
No. of refined parameters	316	388
<i>R</i> _f for significant reflections ^a	0.0625	0.0283
<i>R</i> _w for significant reflections ^b	0.1749	0.0469
Goodness-of-fit ^c	1.300	1.21

$$^a R_f = [\sum(F_o - F_c)/\sum F_o]$$

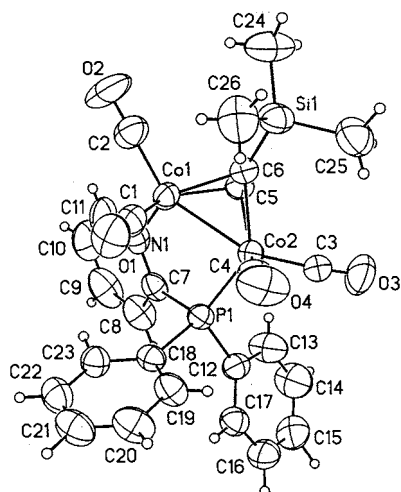
$$^b R_w = \sum w^{1/2}(F_o - F_c)/\sum w^{1/2}F_o$$

$$^c \text{GoF} = [\sum w(F_o - F_c)^2 / (N_{\text{reflns}} - N_{\text{params}})]^{1/2} \quad w^{-1} = \sigma^2(F) + 0.0010F^2$$

Several greenish–brown crystals of **1a** were obtained from the solvent diffusion method. Its structure was determined by X-ray crystallographic methods. It shows that two cobalt atoms are both coordinated by the phosphorus atom and the nitrogen atom of the PPh_2py ligand, respectively (Fig. 1). It is rather unusual for a nitrogen atom, which is classified as a hard base according to the HSAB principle, to coordinate to a low-valence and soft Lewis acid such as Co(0) atom. The stability of this coordination might attribute to the chelate effect of the bidentate ligand, diphenyl-2-pyridylphosphine [8]. The bond length of Co(1)–Co(2) is 2.448 Å. It is slightly shorter than most of the dicobalt compounds with mono-dentate ligands [1a.g].



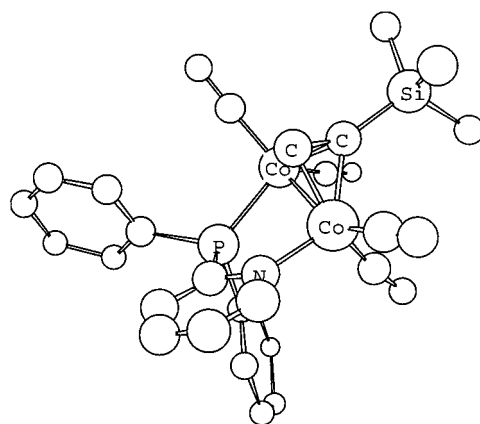
Scheme 2.

Fig. 1. ORTEP drawing with the numbering scheme of **1a**.

The distance between the phosphorus atom and the nitrogen atom is 2.675 Å, which is longer than the bond length of Co(1)–Co(2) (Table 2). The four atoms, N, Co(1), Co(2) and P, are not on the same plane. The dihedral angle of N–Co(1)–Co(2)–P is 25.9°. The bond lengths of Co(1)–N and Co(2)–P are 2.054 and 2.185 Å, respectively. The bond lengths of Co(2)–P is slightly shorter than most of the mono-dentate phosphine cases [1a,g]. Four CO ligands are in different environments because of the asymmetric nature of this binding geometry and the inability of free rotation of the

Table 2
Selected bond lengths (Å) and bond angles (°) for (**1a**)

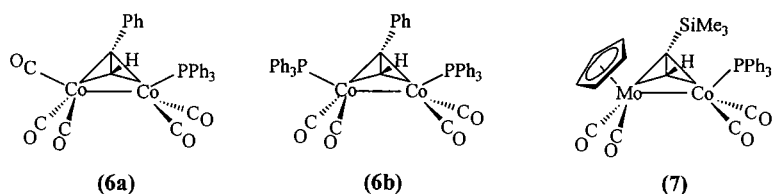
Bond lengths (Å)			
Co(1)–C(5)	1.945(7)	Co(1)–C(6)	2.005(7)
Co(1)–N(1)	2.054(6)	Co(1)–Co(2)	2.4489(13)
Co(2)–C(5)	1.972(7)	Co(2)–C(6)	1.993(7)
Co(2)–P(1)	2.185(2)	P(1)–C(18)	1.833(7)
P(1)–C(7)	1.838(7)	P(1)–C(12)	1.838(7)
Si(1)–C(6)	1.837(8)	N(1)–C(7)	1.337(9)
N(1)–C(11)	1.354(9)	C(5)–C(6)	1.327(10)
Bond angles (°)			
C(2)–Co(1)–C(1)	98.0(4)	C(2)–Co(1)–C(5)	107.2(3)
C(1)–Co(1)–C(5)	140.8(3)	C(2)–Co(1)–C(6)	100.9(4)
C(1)–Co(1)–C(6)	107.5(3)	C(5)–Co(1)–C(6)	39.2(3)
C(2)–Co(1)–N(1)	102.2(4)	C(1)–Co(1)–N(1)	108.3(3)
C(5)–Co(1)–N(1)	95.4(3)	C(6)–Co(1)–N(1)	133.7(3)
C(2)–Co(1)–Co(2)	152.8(3)	C(1)–Co(1)–Co(2)	93.6(2)
C(5)–Co(1)–Co(2)	51.8(2)	C(6)–Co(1)–Co(2)	52.0(2)
N(1)–Co(1)–Co(2)	97.3(2)	C(3)–Co(2)–P(1)	101.7(3)
C(4)–Co(2)–P(1)	105.6(2)	C(5)–Co(2)–P(1)	106.9(2)
C(6)–Co(2)–P(1)	135.4(2)	P(1)–Co(2)–Co(1)	84.55(6)
C(18)–P(1)–C(7)	100.6(3)	C(18)–P(1)–C(12)	104.1(3)
C(6)–Si(1)–C(25)	108.5(4)	C(6)–Si(1)–C(26)	111.5(4)
C(7)–N(1)–Co(1)	120.1(5)	C(6)–C(5)–Co(1)	72.8(4)
C(6)–C(5)–Co(2)	71.3(4)	Co(1)–C(5)–Co(2)	77.4(2)
C(5)–C(6)–Si(1)	147.6(6)	N(1)–C(7)–P(1)	114.1(5)
C(8)–C(7)–P(1)	123.3(6)		

Fig. 2. Aerial view of **1a** along the Co(1)–Co(2) axis.

M(CO)₂(L) fragment. It is also evidenced by the observation of four broad peaks in ¹³C-NMR for these COs. The broad peaks are partly due to the coupling with their attached cobalts ($I = 7/2$). The fact that two phenyl rings are in different chemical environments was supported by two distinct sets of ¹³C-NMR signals of **1a**. The bond angles of C(5)≡C(6)–Si(1) and C(6)≡C(5)–H are 147.5 and 151.3°, respectively. The fact that two substituents bend away from two metal centers is consistent with the common observation for this type of alkyne-bridged binuclear metal compounds [9]. The ³¹P-NMR spectra of **1a** and **1b** are 56.1 and 53.9 ppm, respectively. There are large downfield chemical shifts of phosphorus atoms from their free ligand [10].

The fact that the bulky bidentate ligand and the bulky SiMe₃ group are on different sides of the dicobalt center is clearly shown in Fig. 2. It is so arranged that to prevent the steric hindrance. There is no structural information for **1b**. However, it is proposed that the phosphorus atom, instead of the nitrogen atom, of the PPh₂Py ligand coordinates to the Co(0). In doing so, the prediction of the HSAB principle might be followed. A large downfield chemical shift of the phosphorus atom in ³¹P-NMR spectrum for **1b** supports the supposition. Another favorable evidence comes from the comparison between the ¹H-NMR spectra of **1a**, **1b** and the free ligand. One distinct downfield chemical shift peak, the proton next to nitrogen atom in pyridine, was observed for both **1b** and the free ligand. On the contrary, it was absent in **1a**. This is convincing evidence which indicates the coordination of pyridyl to metal in **1a**, but not in **1b**.

Structural data for several **1b**-related compounds, **6a**, **6b** [11] and **7** [12], are available. The PPh₃ ligands are on the same side of the bridged alkyne for all three cases. It is quite different from the binding pattern of the bidentate ligand, PPh₂Py, in **1a**. The differences will be attributed to the bidentate nature of the PPh₂Py

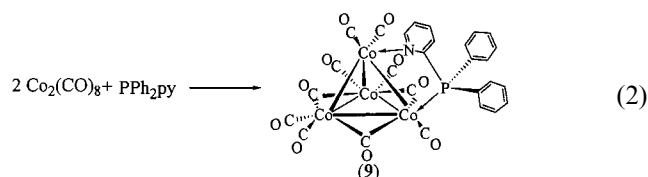
Fig. 3. Selected **1b**-related compounds.

ligand. In the case of **1a**, no free rotation of the bidentate ligand is possible. However, in the cases of monodentate-ligand-coordinated bimetallic compounds, a free rotation of the pseudo-trident fragment $\text{Co}(\text{CO})_2(\text{PPh}_3)$ is possible in solution. It is evidenced by the observation of three equivalent phenyl rings from the ^{13}C -NMR spectra (Fig. 3).

Spectroscopic data, such as ^1H -, ^{13}C - and ^{31}P -NMR spectra, for several selected bridged compounds are listed in Table 3 for comparison. A distinguished downfield shift for **1a** in ^1H -NMR spectrum implies that the acetylenic proton bends away from the dicobalt metal center with large angle. The largest downfield shift in ^{31}P -NMR spectrum for **1a** also indicates that the diphenyl-2-pyridylphosphine ligand donates more electron density to the metal center than other compounds.

Several selected reactions with different ratios of $\text{Co}_2(\text{CO})_8/\text{TMSA}$ in the presence or absence of the phosphine ligands were pursued. All these reactions were carried out in the same reaction conditions. The results are shown in Table 4 for comparison. As mentioned, **4** can be obtained quantitatively from the oxidation of **3**. Here below, the summation of the yields of **3** and **4** is used as an indicator for the efficiency of the reaction. By that criterion, Entry 3 represents the best reaction condition among the first three entries. To our surprise, not only **4** but also **3** was observed in the reaction (Entries 4 and 5) and the yields were fair. The reason that **3** was absent arises from the steric hindrance of bidentate $\mu\text{-}P,N\text{-PPh}_2\text{py}$ and monodentate PPh_2py ligands. It seems reasonable to say that the presence of the PPh_2py ligand enhances the formation of **3** and **4**.

It has been known that tetracobalt compound, $\text{Co}_4(\text{CO})_{12}$, could be obtained from heating $\text{Co}_2(\text{CO})_8$ in solution [13]. The reaction of $\text{Co}_2(\text{CO})_8$ with diphenyl-2-pyridylphosphine was carried out in toluene at 80°C for 4 h. It yielded one major compound, $\text{Co}_4(\text{CO})_{10}(\mu\text{-}P,N\text{-PPh}_2\text{py})$ (**9**) (Eq. (2)).



The structure of **9** was determined by X-ray crystallographic methods. The P and N atoms of PPh_2py are coordinated to the basal and apical position of the tetracobalt cluster, respectively (Fig. 4). The apical cobalt atom is harder than that of the basal cobalt atoms, probably due to the electron diffusing capacity of the bridging COs [14]. The bond length of $\text{Co}(1)\text{--Co}(2)$ is 2.493 Å; it is 2.686 Å for the P, N distance (Table 5). Four atoms, N, $\text{Co}(1)$, $\text{Co}(2)$ and P, are not on the same plane; the dihedral angle of $\text{N--Co}(1)\text{--Co}(2)\text{--P}$ is 33.5° . The bond lengths of $\text{Co}(1)\text{--N}$ and $\text{Co}(2)\text{--P}$ are 2.053 and 2.183 Å, respectively. The corresponding bond lengths and angles of **1a** and **9** are very similar. This is attributed to the rigidity of the bidentate ligand, $\mu\text{-}P,N\text{-PPh}_2\text{py}$.

Three bridging COs in solid state are clearly seen from another view of **9**. IR spectroscopy also shows bridging carbonyl stretching frequencies around 1800 cm^{-1} . However, there is no bridging as well as terminal CO signal observed in the ^{13}C -NMR spectrum. This suggests that all COs might be fluxional in solution at room temperature (Fig. 5) [15].

3. Experimental

All operations were performed in a nitrogen-flushed glove box or in a vacuum system. Freshly distilled solvents were used. All processes of separation of the products were performed by centrifugal thin-layer chromatography (TLC, Chromatotron, Harrison model 8924). ^1H -, and ^{13}C -NMR spectra were recorded by a Varian VXR-400S spectrometer at 400.45 and 100.70

Table 3
Chemical shifts of selected alkyne-bridged compounds

Compound	^1H -NMR ^a	^{13}C -NMR ^b	^{31}P -NMR
Chemical shift δ (ppm)			
1a	6.29 (d, $J_{\text{PH}} = 5.2$ Hz)	90.9, 93.1	56.1
1b	5.64 (d, $J_{\text{PH}} = 6.2$ Hz)	73.9, 86.2	53.9
6a	5.45 (d, $J_{\text{PH}} = 3.8$ Hz)	71.2, 86.0	51.6
6b	4.53 (t, $J_{\text{PH}} = 3.0$ Hz)	70.8, 81.9	50.4
7	5.25 (d, $J_{\text{PH}} = 10$ Hz)	89.8, 95.0	54.7

^a Acetylenic proton.

^b $\text{HC}\equiv\text{CSiMe}_3$.

Table 4
Reactions of $\text{Co}_2(\text{CO})_8$ with TMSA in the presence/absence of phosphine ligand ^a

Entry	Reactant	Equation of TMSA	Ligand	Product (%)			
				3	4	3+4	8 ^b
1	$\text{Co}_2(\text{CO})_8$	10	–	15.9	5.0	20.9	–
2	$\text{Co}_2(\text{CO})_8$	10	PPh_3	45.3	1.9	47.2	51.1
3	$\text{Co}_2(\text{CO})_8$	10	PPh_2py	64.0	21.7	85.7	–
4	1a	9	–	–	31.6	31.6	–
5	1b	9	–	–	35.7	35.7	–

^a All these reactions were carried out in 20 ml THF at 60°C for 12 h.

^b $\text{Co}_2(\text{CO})_5(\text{PPh}_3)(\mu\text{-HC}\equiv\text{CSiMe}_3)$.

MHz, respectively, while some ^{13}C - and ^{31}P -NMR spectra were recorded by a Varian VXR-300S spectrometer at 75.46 and 121.42 MHz, respectively; chemical shifts are reported in ppm relative to internal TMS. Mass spectra were recorded on a Joel JMS-SX/SX 102A GC/MS/MS spectrometer. Elemental analysis were recorded on a Heraeus CHN-O-S-Rapid.

3.1. Preparations of **1a** and **1b**

Into a 100 cm³ flask was placed dicobalt octacarbonyl, $\text{Co}_2(\text{CO})_8$, (0.6 g, 1.75 mmol), trimethylsilylacetylene (0.38 ml, 2.69 mmol) and diphenyl-2-pyridylphosphine (0.462 g, 1.75 mmol) with 30 cm³ of THF. The solution was stirred at 60°C for 7 h.

Subsequently, the resulting dark purple solution was filtered through a small amount of silica gel. The filtrate was evaporated under reduced pressure to yield the crude product. Purification with centrifugal thin-layer chromatography was carried out. The first three bands were eluted with hexane. A trace amount of brown band was characterized as the known compound, $\text{Co}_2(\text{CO})_6\{\mu\text{-HC}\equiv\text{CSiMe}_3\}$ (**2**). The second band was identified as the known compound, 2,5-bis(trimethylsilyl)cyclopenta-2,4-dien-1-one (**4**) with 10% yield. The third band is greenish brown and was characterized as $\text{Co}_2(\text{CO})_4(\mu\text{-}P,N\text{-PPh}_2\text{py})\{\mu\text{-HC}\equiv\text{CSiMe}_3\}$ **1a**. The yield of **1a** is 15% based on the amount of $\text{Co}_2(\text{CO})_8$ being used in the reaction. The fourth band was eluted with mixture solvent (3:2 hexane– CH_2Cl_2). It was characterized as $\text{Co}_2(\text{CO})_5(\text{PPh}_2\text{Py})(\mu\text{-HC}\equiv\text{CSiMe}_3)$ (**1b**). The yield of **1b** is 15%. The last band was eluted with CH_2Cl_2 and found $\text{Co}_2(\text{CO})_2(\mu\text{-CO})_2(\eta^4\text{-}2,5\text{-bistrimethylsilylcyclopentadienone})_2$ (**3**) with 15% yield.

3.2. Characterization of **1a** and **1b**

3.2.1. Characterization of $\text{Co}_2(\text{CO})_4(\mu\text{-}P\text{Ph}_2\text{Py})(\mu\text{-HC}\equiv\text{CSiMe}_3)$ (**1a**)

$^1\text{H-NMR}(\text{CDCl}_3)$: δ 0.14(s, 9H, SiMe_3), 6.29(d, $J=5.2$, 1H, CH), 6.92(d, $J=7.2$, 1H, pyridine), 7.15(t, 1H, pyridine), 7.26–7.41(m, 10H, arene), 7.51(t, 1H,

pyridine), 8.98(d, $J=4$, 1H, pyridine); $^{13}\text{C-NMR}(\text{CDCl}_3)$: δ 0.73(s, 3C, SiMe_3), 90.90(s, 1C, C– SiMe_3), 93.12(s, 1C, CH), 124.19(s, 1C, pyridine), 128.44(d, $J=8.4$, 2C, arene), 128.52(s, $J=6.9$, 2C, arene), 129.50(s, 1C, *p*-arene), 129.73(s, 1C, *p*-arene), 131.85(d, $J=19.0$, 2C, arene), 131.98(d, $J=19.8$, 2C, arene), 134.70(s, 1C, pyridine), 136.51(d, $J=77.0$, 1C, *ipso* of arene), 136.85(d, $J=80.9$, 1C, *ipso* of arene), 154.50(d, $J=13.0$, 1C, pyridine), 166.60(d, $J=62.5$, 1C, pyridine), 202.6(m, CO), 203.1(m, CO), 204.9(m, CO), 206.6(m, CO); $^{31}\text{P-NMR}(\text{CDCl}_3)$: δ 56.1; Elemental analysis: Anal. Calc. C, 52.80; H, 4.06; N, 2.37; found C, 52.55; H, 4.27; N, 2.65; MS: m/z 563 [P-CO^+]; IR (CH_2Cl_2): $\nu(\text{CO})$ 2054(m), 2055(sh), 1983(s), 1953(s).

3.2.2. Characterization of $\text{Co}_2(\text{CO})_5(\text{PPh}_2\text{Py})(\mu\text{-HC}\equiv\text{CSiMe}_3)$ (**1b**)

$^1\text{H-NMR}(\text{CDCl}_3)$: δ 0.01(s, 9H, SiMe_3), 5.64(d, $J=6.4$, 1H, CH), 7.26(1H, pyridine), 7.32(t, 1H, pyridine), 7.41(6H, arene), 7.54(t, 4H, arene), 7.62(t, 1H,

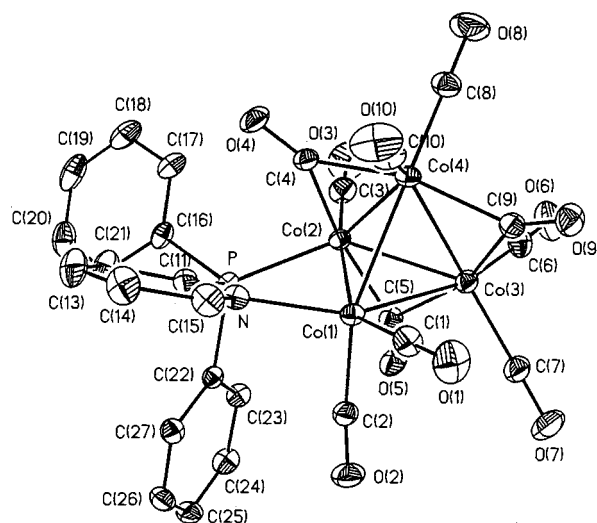


Fig. 4. ORTEP drawing with the numbering scheme of **9**. Hydrogen atoms were omitted for clarity.

Table 5
Selected bond lengths (Å) and bond angles (°) for **9**

Bond lengths (Å)			
Co(1)–Co(2)	2.493(1)	Co(1)–Co(4)	2.543(1)
Co(1)–Co(3)	2.530(1)	Co(1)–N	2.053(3)
Co(2)–Co(4)	2.480(1)	Co(2)–Co(3)	2.457(1)
Co(2)–C(3)	1.782(4)	Co(2)–C(4)	1.940(3)
Co(2)–C(5)	1.879(3)	Co(2)–P	2.183(1)
Co(4)–Co(3)	2.442(1)	C(1)–O(1)	1.129(5)
C(4)–O(4)	1.150(4)	P–C(11)	1.840(3)
P–C(16)	1.841(3)	P–C(22)	1.819(3)
N–C(11)	1.344(4)	N–C(15)	1.337(5)
Bond angles (°)			
Co(2)–Co(1)–Co(4)	59.0(1)	C(1)–Co(1)–C(2)	94.4(2)
Co(2)–Co(1)–N	94.2(1)	Co(4)–Co(1)–N	103.7(1)
Co(3)–Co(1)–N	151.7(1)	C(1)–Co(1)–N	105.1(1)
C(2)–Co(1)–N	99.3(1)	C(3)–Co(2)–C(5)	94.4(2)
Co(1)–Co(2)–P	83.4(1)	Co(4)–Co(2)–P	125.7(1)
Co(3)–Co(2)–P	137.1(1)	C(3)–Co(2)–P	103.3(1)
C(4)–Co(2)–P	88.2(1)	C(5)–Co(2)–P	101.0(1)
Co(1)–C(1)–O(1)	173.7(4)	Co(2)–C(4)–Co(4)	79.9(1)
Co(2)–C(4)–O(4)	141.9(3)	Co(2)–P–C(11)	108.4(1)
Co(2)–P–C(16)	118.3(1)	C(11)–P–C(16)	103.7(1)
Co(2)–P–C(22)	120.1(1)	C(11)–P–C(22)	102.0(1)
C(16)–P–C(22)	102.1(1)	Co(1)–N–C(11)	119.8(2)
Co(1)–N–C(15)	122.0(2)	C(11)–N–C(15)	118.2(3)
P–C(11)–N	114.1(2)	N–C(15)–C(14)	122.7(3)

pyridine), 8.79(d, 1H, pyridine); $^{13}\text{C-NMR}(\text{CDCl}_3)$: δ 1.41(s, 3C, SiMe₃), 73.86(s, 1C, C–SiMe₃), 86.19(s, 1C, CH), 123.30(s, 1C, pyridine), 127.60(d, $J = 21.3$, 1C, pyridine), 128.18(d, $J = 9.9$, 2C, arene), 128.20(d, $J = 9.86$, 2C, arene), 130.01(s, 2C, *p*-arene), 133.32(d, $J = 11.4$, 2C, arene), 133.38(d, $J = 10.7$, 2C, arene), 134.48(d, $J = 39.7$, 1C, *ipso* of arene), 134.66(d, $J = 40.5$, 1C, *ipso* of arene), 135.51(d, $J = 6.8$, 1C, *ipso* of pyridine), 149.87(d, $J = 16.0$, 1C, pyridine), 160.11(d, $J = 62.5$, 1C, pyridine), 201.8(m, 2CO), 205.8(m, 3CO); $^{31}\text{P-NMR}(\text{CDCl}_3)$: $\delta = 53.9$; Elemental Analysis: Anal. Calc. C, 52.35; H, 3.87; N, 2.26; found C, 52.14; H, 3.89; N, 2.4; MS m/z 622 [$\text{P} + 3^+$]; IR(CH₂Cl₂): $\nu_{(\text{CO})}$ 2058(s), 1996(s), 1959(sh).

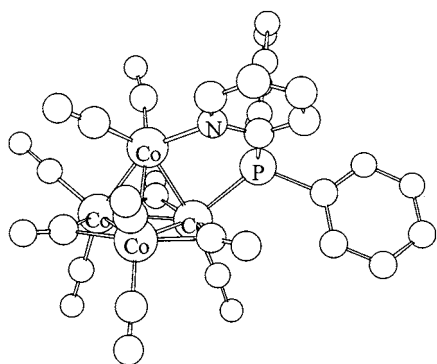


Fig. 5. Aerial view of **9** along the P–Co(2)–Co(1)–P plane.

3.3. Preparation of **9**

Into a 100 cm³ flask was placed dicobalt octacarbonyl, Co₂(CO)₈, (1.2 g, 3.509 mmol) and diphenyl-2-pyridylphosphine (0.462 g, 1.755 mmol) with 30 cm³ of toluene. The solution was stirred at 80°C during the next 4 h.

Subsequently, the resulting dark green solution was filtered through a small amount of silica gel. The following purification procedures for the products are similar to those in Section 3.1. The band of Co₄(CO)₁₀(μ -P,N-PPh₂Py) (**9**) was eluted with CH₂Cl₂ together with a trace amount of unidentified byproduct. The yield of **9** is 68%.

3.3.1. Characterization of Co₄(CO)₁₀(μ -PPh₂Py) (**9**)

$^1\text{H-NMR}(\text{CDCl}_3)$: δ 0.14(s, 9H, SiMe₃), 6.29(d, $J = 5.2$, 1H, CH), 6.92(d, $J = 7.2$, 1H, pyridine), 7.15(t, 1H, pyridine), 7.26–7.41(m, 10H, arene), 7.51(t, 1H, pyridine), 8.98(d, $J = 4$, 1H, pyridine); $^{13}\text{C-NMR}(\text{CDCl}_3)$: δ 125.26(s, 1C, *p*-pyridine), 129.00(d, $J = 9.9$, 1C, pyridine), 131.01(d, $J = 8.5$, 1C, *ipso* of pyridine), 131.27(s, 2C, *p*-arene), 131.91(d, $J = 41.1$, 2C, *ipso* of arene), 133.38(d, $J = 10.7$, 4C, arene), 136.58(d, 4C, arene), 155.42(d, $J = 13.0$, 1C, pyridine), 168.65(d, $J = 63.4$, 1C, pyridine); $^{31}\text{P-NMR}(\text{CDCl}_3)$: δ 38.1; Elemental Analysis: Anal. Calc. C, 41.62; H, 1.81; N, 1.80; found C, 41.79; H, 2.21; N, 2.25; MS m/z 751 [$\text{P}^+ - \text{CO}$]; IR(CH₂Cl₂): $\nu_{(\text{CO})}$ 2066(m), 2055(sh), 2022(s), 1998(sh), 1832(m), 1804(m).

3.4. General procedures for Entries 1, 2, and 3

Dicobalt octacarbonyl, Co₂(CO)₈, (0.2 g, 0.58 mmol) and trimethylsilylacetylene (0.83 ml, 5.87 mmol) were placed in a 100 cm³ flask with 20 cm³ of THF and the corresponding ligand for each entry. They are triphenylphosphine (0.15 g, 0.59 mmol) and diphenyl-2-pyridylphosphine (0.15 g, 0.59 mmol) for Entry 2 and Entry 3, respectively. The solution was stirred at 60°C for 12 h.

The following purification procedures for the desired compounds are similar to those in Section 3.1. The products, **4** and **3**, were eluted out by hexane and CH₂Cl₂, respectively. The yields are listed in Table 4.

3.5. General procedures for Entries 4, and 5

For Entry 4, **1a** (0.374 g, 0.632 mmol) and trimethylsilylacetylene (0.81 ml, 5.74 mmol) with 20 cm³ of THF were placed in a 100 cm³ flask and stirred at 60°C for 12 h. The resulting greenish–brown solution was subjected for purification.

The following purification procedures are similar to those in Section 3.1. The only product of **4** was eluted with hexane.

Similar procedures were used for Entry 5, which employed **1b** (0.144 g, 0.232 mmol) and trimethylsilylacetylene (0.3 ml, 2.12 mmol) as reactants. The resulting dark brown solution was subjected for further purification. Compound **4** is the only isolated product. The yields are listed in Table 4.

3.6. X-ray crystallographic study

Suitable crystals of **1a** and **9** were sealed in thin-walled glass capillaries under nitrogen atmosphere. The crystal of **1a** was mounted on a Siemens Smart CCD diffractometer; the crystal of **9** was mounted on a Siemens P4 diffractometer. The crystallographic data were collected using a $\theta - 2\theta$ scan mode with Mo-K α radiation. The space group determination was based on a check of the Laue symmetry and systematic absences, and was confirmed by the structure solution. The structure was solved by direct methods using Siemens SHELXTL PLUS package [16]. All non-H atoms were located from successive Fourier maps. Anisotropic thermal parameters were used for all non-H atoms and fixed isotropic for H atoms that were refined using riding model [17]. Crystallographic data of **1a** and **9** are summarized in Table 1.

4. Supplementary material available

Atomic coordinates of **1a** and **9**, tables of thermal parameters, bond lengths and angles, anisotropic thermal parameters, and H atom coordinates have been deposited as supplementary material.

Acknowledgements

We thank the National Research Council of the Republic of China (Grant NSC-88-2113-M-005-022) for support.

References

- [1] (a) J. Puddephatt, Chem. Soc. Rev. 12 (1983) 99. (b) J.P. Farr, M.M. Olmstead, N.M. Rutherford, F.E. Wood, A.L. Balch, Organometallics 2 (1983) 1758. (c) J.P. Farr, F.E. Wood, A.L. Balch, Inorg. Chem. 22 (1983) 1229. (d) J.P. Farr, M.M. Olmstead, A.L. Balch, Inorg. Chem. 22 (1983) 3387. (e) Z.-Z. Zhang, H.K. Wang, H.G. Wang, R.J. Wang, J. Organomet. Chem. 314 (1986) 357. (f) Z.-Z. Zhang, H.-K. Wang, Z. Xi, X.-K. Yao, R.-J. Wang, J. Organomet. Chem. 376 (1989) 123. (g) Z.-Z. Zhang, H. Cheng, Coord. Chem. Rev. 147 (1996) 1.
- [2] (a) K. Kurtev, D. Ribola, R.A. Jones, D.J. Cole-Hamilton, G. Wilkinson, J. Chem. Soc. Dalton Trans. (1980) 55. (b) E. Linder, H. Rauleder, P. Wegner, Naturforschung B39 (1984) 1224.
- [3] (a) M. Maekawa, M. Munakata, S. Kitagawa, T. Yonezawa, Bull. Chem. Soc. Jpn. 64 (1991) 2286. (b) E. Lastra, M.P. Gamasa, J. Gimeno, M. Lanfranchi, A. Tiripicchio, J. Chem. Soc. Dalton Trans. (1989) 1499. (c) N.W. Alcock, P. Moore, P.A. Lampe, K.F. Mok, J. Chem. Soc. Dalton Trans. (1982) 207. (d) C.-H. Su, M.Y. Chiang, J. Chin. Chem. Soc. 44 (1997) 539.
- [4] (a) R.G. Pearson, J. Am. Chem. Soc. 85 (1963) 3533. (b) R.G. Pearson (Ed.), Hard and Soft Acids and Bases, Dowden, Hutchinson and Ross, Stroudsburg, 1973. (c) R.G. Pearson, Chemical hardness, in: K. Sen (Ed.), Structural Bonding 80 (1993) 1.
- [5] (a) T.-Y. Luh, Coord. Chem. Rev. 60 (1984) 255. (b) R.J. Baxter, G.R. Knox, P.L. Pauson, M.D. Spicer, Organometallics 18 (1999) 197. (c) R.J. Baxter, G.R. Knox, J.H. Moir, P.L. Pauson, M.D. Spicer, Organometallics 18 (1999) 206.
- [6] (a) R.D.W. Kemmitt, D.R. Russell, in: G. Wilkinson, F.G.A. Stone, E.W. Abel (Eds.), Comprehensive Organometallic Chemistry, vol. 5, Pergamon, Oxford, 1982. (b) M.J. Chetcuti, in: E.W. Abel, F.G.A. Stone, G. Wilkinson (Eds.), Comprehensive Organometallic Chemistry II, vol. 10, Elsevier Science, New York, 1995, pp. 44. (c) M.J. Chetcuti, P.E. Fanwick, J.C. Gordon, Inorg. Chem. 30 (1991) 4710. (d) G. Gervasio, E. Sappa, L. Markó, J. Organomet. Chem. 444 (1993) 203. (e) O.S. Mills, G. Robinson, Proc. Chem. Soc. (1964) 187. (f) F.S. Stephens, Acta Crystallogr. Sect. A Cryst. Phys. Diffr. Theor. Gen. Crystallogr. 154 (1966) 21A. (g) F.-E. Hong, J.-Y. Wu, Y.-C. Huang, C.-K. Hung, H.-M. Gau, C.-C. Lin, J. Organomet. Chem. 580 (1999) 98.
- [7] The yield of **3** is about 25%.
- [8] A.L. Balch, in: M.H. Chisholm (Eds.), Reactivity of Metal–Metal Bonds, American Chemical Society, 1981, pp. 167.
- [9] (a) L.S. Hegedus, Transition Metals in the Synthesis of Complex Organic Molecules, University Science Books, Mill Valley, CA, 1994 (Chapter 8). (b) R.S. Dickson, Adv. Organomet. Chem. 12 (1974) 323. (c) R.S. Dickson, G.R. Tailby, Aust. J. Chem. 23 (1971) 229. (d) U. Krücker, W. Hübel, Chem. Ber. 94 (1961) 2829.
- [10] The ^{31}P -NMR peak for PPh_2py occurs at -3.9 ppm.
- [11] Unpublished results.
- [12] F.-E. Hong, C.-K. Hung, C.-C. Lin, J. Chin. Chem. Soc. 44 (1997) 43.
- [13] (a) C.R. Eady, B.F.G. Johnson, J. Lewis, J. Chem. Soc. Dalton Trans. (1975) 2606. (b) F. Ungvary, L. Markó, J. Organomet. Chem. 71 (1974) 283.
- [14] C.M. Lukehart, Fundamental Transition Metal Organometallic Chemistry, Brooks/Cole, Monterey, CA, 1985 (Chapter 3).
- [15] B.F.G. Johnson, A. Rodgers, in: D.F. Shriver, H.D. Kaesz, R.D. Adams (Eds.), The Chemistry of Metal Cluster Complexes, VCH, 1990 (Chapter 6).
- [16] G.M. Sheldrick, SHELXTL PLUS User's Manual. Revision 4.1 Nicolet XRD Corporation, Madison, WI, 1991.
- [17] The hydrogen atoms were riding on carbons or oxygens in their idealized positions and held fixed with C–H distances of 0.96 Å.